

Supplemental Information

An Inherently Bifunctional Subset of Foxp3⁺ T Helper Cells Is Controlled by the Transcription Factor Eos

**Madhav D. Sharma, Lei Huang, Jeong-Hyeon Choi, Eun-Joon Lee, James M. Wilson,
Henrique Lemos, Fan Pan, Bruce R. Blazar, Drew M. Pardoll, Andrew L. Mellor,
Huidong Shi, and David H. Munn**

Supplemental Inventory

1. Supplemental Figures

Figure S1, Related to Figure 1

Figure S2, Related to Figure 2

Figure S3, Related to Figure 3

Figure S4, Related to Figure 4

Figure S5, Related to Figure 5

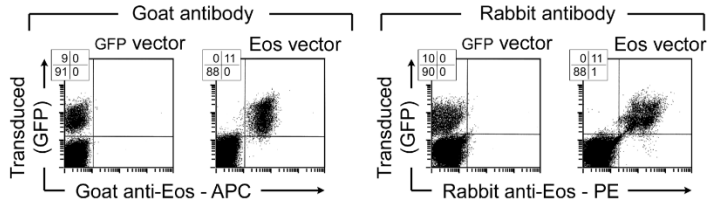
Figure S6, Related to Figure 6

Figure S7, Related to Figure 7

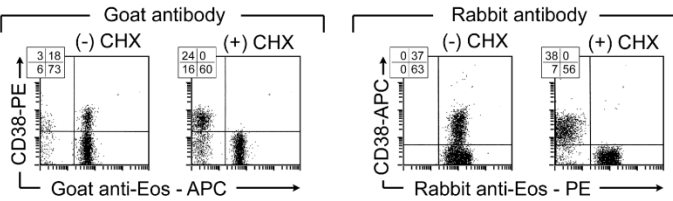
2. Supplemental Experimental Procedures

3. Supplemental References

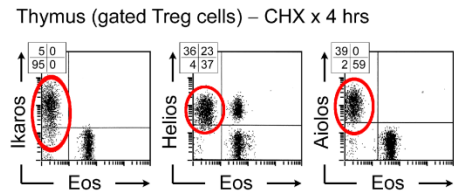
A Transfected 3T3 cells



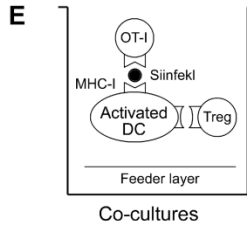
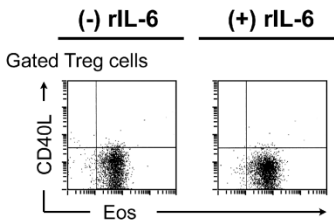
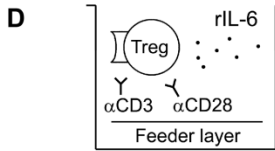
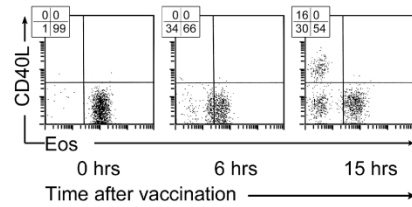
Thymus - 4 hr CHX assay (gated Treg cells)



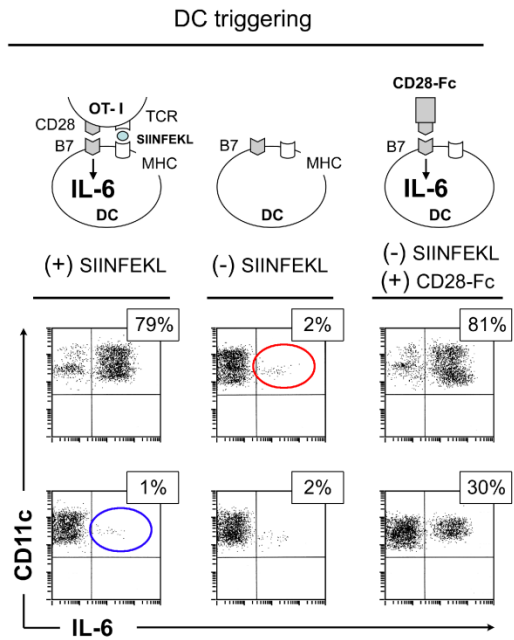
B Cross-reactivity testing:



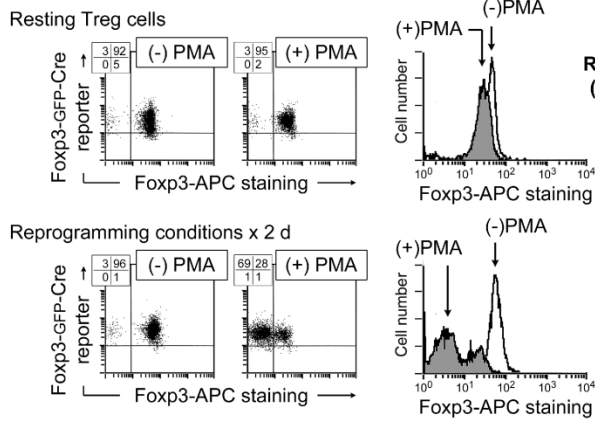
C Gated Treg cells (CD4⁺GFP⁺)



Activated DCs (tumor-draining LN)



F



Treg cells (after reprogramming conditions x 3 days)

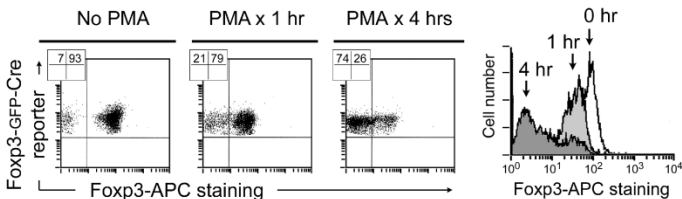


Figure S1. Downregulation of Eos in Reprogrammed Treg Cells, Related to Figure 1

(A) Validation of intracellular FACS staining using two different Eos antibodies.

(upper panels) The 3T3 fibroblast cell line (normally Eos-negative) was transduced with either Eos-GFP vector or control (empty GFP) vector, then stained for intracellular Eos expression with two different commercial polyclonal antibodies (goat and rabbit), raised against two different peptides. Both antibodies reacted with the Eos-transduced 3T3 cells, but not with the control-transduced cells. **(lower panels)** Thymic cells were treated for 4 hrs with cycloheximide (CHX) to disclose the Eos-labile population (defined as loss of Eos after CHX treatment), then stained for CD38 (a marker for the Eos-labile Treg cell subset) vs. intracellular Eos, using the two different goat and rabbit Eos antibodies. Gated Treg cells are shown. The data are taken from two separate experiments, using independent markers to identify the Treg cells. In each case the Eos antibody reacted exclusively with the Foxp3⁺ Treg cells, and both Eos antibodies identified the same population of CD38⁺ Treg cells that uniformly expressed Eos before CHX, and selectively downregulated Eos after CHX. Likewise, both antibodies showed that the CD38^{NEG} Treg cells (the “Eos-stable” subset) expressed unchanged Eos irrespective of CHX. (The appearance of the CD38 staining differs slightly because the antibodies are in different fluorochrome conjugates.) Goat anti-Eos was used in subsequent experiments unless otherwise noted.

(B) The Eos antibody is not cross-reactive with other Ikaros-family members. Thymocytes from *Foxp3*^{GFP} mice were treated for 4 hrs with CHX to induce loss of Eos in the Eos-labile subset. Cells were then stained for Eos (goat polyclonal antibody) vs. each of the other Ikaros family members (Ikaros, Helios and Aiolos). In each plot, the red circle indicates those Treg cells that stained positive for the other Ikaros-family member but were negative for Eos. The existence of these single-positive cells shows that the Eos antibody was not cross-reactive with that particular family member (because if the Eos antibody were cross-reactive there could not be any such cells, since all cells that were positive for the other family-member would have also bound the cross-reactive Eos antibody). The figure shows that some Treg cells were authentically dual-positive for both Eos and Helios. Many T cells express Ikaros, Helios or Aiolos during differentiation, so dual-positive cells are expected (Avitahl et al., 1999; Quintana et al., 2012; Thornton et al., 2010). However, to rule out cross-reactivity, the informative cells are the Helios⁺Eos^{NEG} population.

(C) Time-course for Eos downregulation in VDLNs in vivo. *Foxp3*^{GFP} mice received OT-I cells followed by vaccination with OVA protein + CpG in IFA, as in manuscript Figure 1A. After 0, 6 or 15 hrs the VDLNs were harvested and stained for intracellular Eos and surface CD40L.

(D) Recombinant IL-6 alone is not sufficient to drive reprogramming. Sorted Foxp3-GFP⁺ Treg cells were activated in vitro using conventional (non-reprogramming) conditions comprising anti-CD3+anti-CD28 mitogen plus T-depleted spleen cells, as described by Shevach and co-workers (Thornton and Shevach, 2000). Cultures received either recombinant IL-6 (20 ng/ml) or vehicle control. After 4 days Treg cells were stained for Eos vs CD40L.

(E) Activated effector cells are required to trigger expression of IL-6 by DCs. Resting DCs were isolated from LNs of untreated mice. Activated DCs were sorted from either tumor-draining LNs (TDLNs) or VDLNs and used in reprogramming co-cultures. In experiments using TDLN DCs, which express high levels of IDO, co-cultures also received the IDO inhibitor 1MT (200 μ M) to allow reprogramming. All co-cultures received OT-I effector T cells, Treg cells and

feeder layer, as described in manuscript Figure 1C, with or without SIINFEKL antigen as indicated. To mimic the CD28→B7 signal delivered during antigen presentation, some cultures received CD28-Fc fusion-protein (the extracellular domain of CD28 ligated to the immunoglobulin Fc domain (Orabona et al., 2004)). After 2 days the DCs were stained for intracellular IL-6. In the case of activated DCs (upper row), adding SIINFEKL antigen triggered robust expression of IL-6 (percentages give the proportion of IL-6-expressing DCs in each treatment group). In contrast, in the absence of SIINFEKL there was no expression of IL-6 (red circle). Thus, some signal associated with antigen presentation appeared required for IL-6 induction. We hypothesized that this signal might be CD28-mediated ligation of B7 molecules (Orabona et al., 2004). Consistent with this hypothesis, the effect of SIINFEKL could be fully replaced by adding CD28-Fc fusion protein to artificially ligate B7 molecules on the DCs. In contrast to the activated DCs, resting DCs did not express IL-6 in response to antigen-activated OT-I (blue circle). The potent stimulus of recombinant CD28-Fc could drive some IL-6 expression even in resting DCs, but this was less than in activated DCs.

(F) Artifactual loss of intracellular antibody access to Foxp3 in reprogrammed Treg cells after PMA activation. Without activation, splenic Treg cells from *Foxp3*^{GFP-Cre} reporter mice were found to have good concordance between the GFP reporter gene and intracellular Foxp3 antibody staining in virtually all Treg cells (upper row; the dot-plots show gated Treg cells from co-cultures similar to the panel S1E, without any SIINFEKL activation). In these resting Treg cells (not exposed to reprogramming conditions) subsequent treatment with PMA+ionomycin + brefeldin A for 4 hrs (the protocol we normally used for intracellular cytokine staining) had no effect on antibody detection of Foxp3. However, when Treg cells had been previously exposed to reprogramming conditions in co-cultures (middle row), then PMA treatment caused a rapid artifactual loss of antibody staining for Foxp3 in many of the Treg cells (even though the cells remained uniformly positive for the GFP reporter gene, and had all been positive for Foxp3 by antibody staining immediately before the PMA treatment, as shown in the left-hand dot-plot). The bottom row shows a time-course for artifactual loss of Foxp3 antibody staining after PMA. Histograms show the superimposed data from all 3 dot-plots.

These findings are consistent with our previous report (Sharma et al., 2010). In general, we found that any extensive manipulation of Treg cells after exposure to reprogramming conditions could contribute to artifactual loss of the Foxp3 staining signal. Therefore, in the current report, we used brief staining times, minimized the manipulation of the Treg cells, and avoided PMA treatment when staining for Foxp3. The cause of this technical artifact is unknown, but may reflect subcellular redistribution of Foxp3 or sequestration within multi-protein complexes (Rudra et al., 2012), that restricts access of the staining antibody.

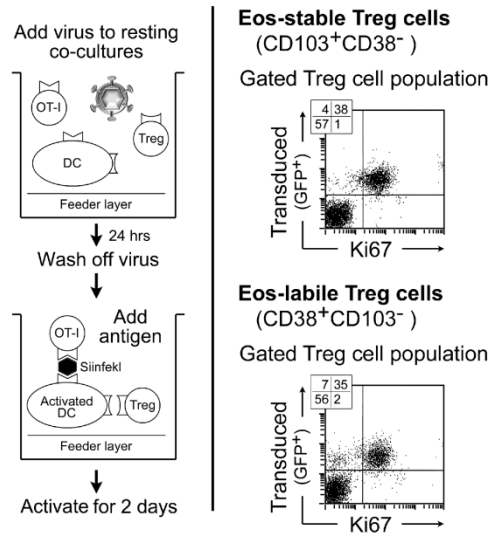


Figure S2. Preferential Transduction of Ki67⁺ Treg Cells by MSCV Vector, Related to Figure 2

Virus supernatants were prepared from producer cells containing pMig (MSCV-IRES-GFP) virus vector. C57Bl/6 splenic Treg cells (CD4⁺CD25⁺) were sorted into Eos-stable (CD103⁺CD38^{NEG}) and Eos-labile (CD38⁺CD103^{NEG}) populations. Sorted Treg cell subsets were incubated overnight with MSCV virus vector (control, GFP-only) in resting, un-activated co-cultures (containing Treg cells, VDLN DCs and OT-I, but without SIINFEKL antigen) in the presence of polybrene, as described in the Supplemental Experimental Procedures. Supernatant was then washed off, fresh medium and SIINFEKL added, and cultures continued for 2 days. Treg cells were efficiently transduced under this protocol, and the successfully transduced Treg cells were almost entirely those that were in cell-cycle (Ki67⁺). Both Eos-stable and Eos-labile Treg cell subsets had similar transduction efficiencies.

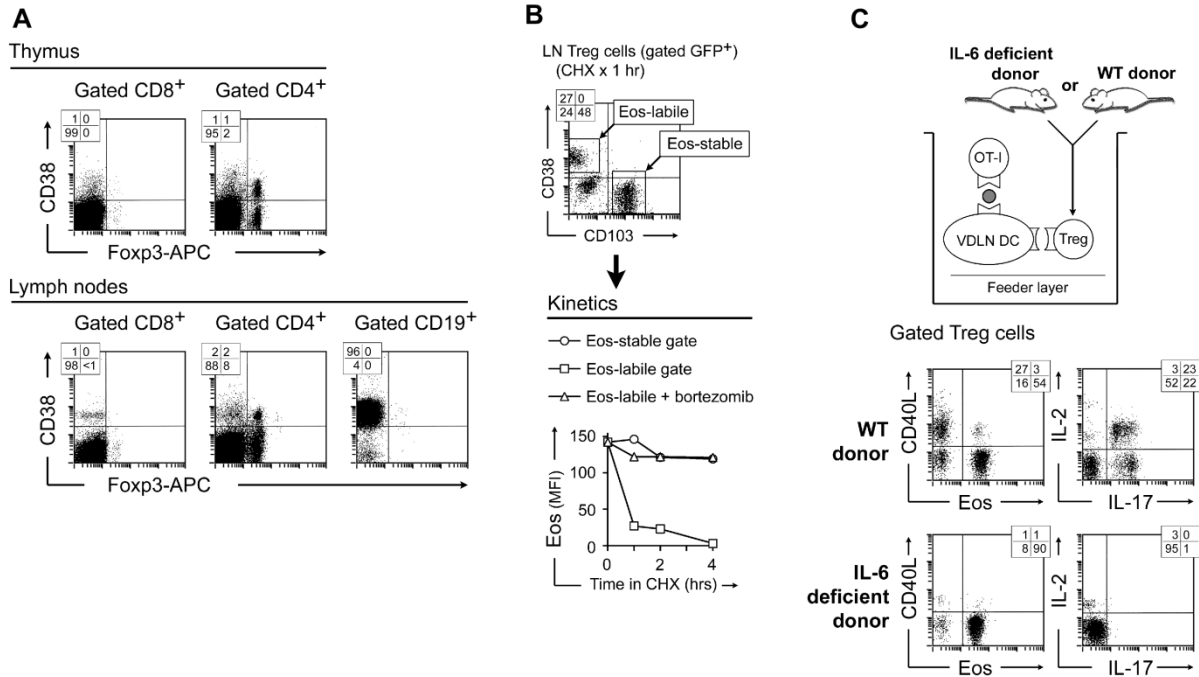


Figure S3. Markers for the Eos-Labile Phenotype, Related to Figure 3

(A) Pattern of expression of the CD38 marker in thymus and LNs. Thymus and LN cells were stained for Foxp3 and CD38 versus CD8, CD4 or CD19 as shown. All cell populations showed the pattern of CD38 staining expected from the literature (Malavasi et al., 2008).

(B) Eos-labile Treg cells in the periphery. Peripheral LN cells from *Foxp3*^{GFP} mice were incubated for 0-4 hrs with CHX, or CHX plus 10 uM bortezomib. Eos expression (mean fluorescence) is graphed separately for each gated sub-population.

(C) Treg cells from IL-6 deficient mice fail to undergo reprogramming in vitro. Splenic Treg cells (CD4⁺CD25⁺) were sorted from either WT B6 mice or IL-6 deficient mice (*Il6*^{-/-}), then tested in reprogramming assays as described in manuscript Figure 1C. All other cells in the co-cultures derived from WT B6 donors. After 2 days, the Treg cells were analyzed for loss of Eos and evidence of reprogramming.

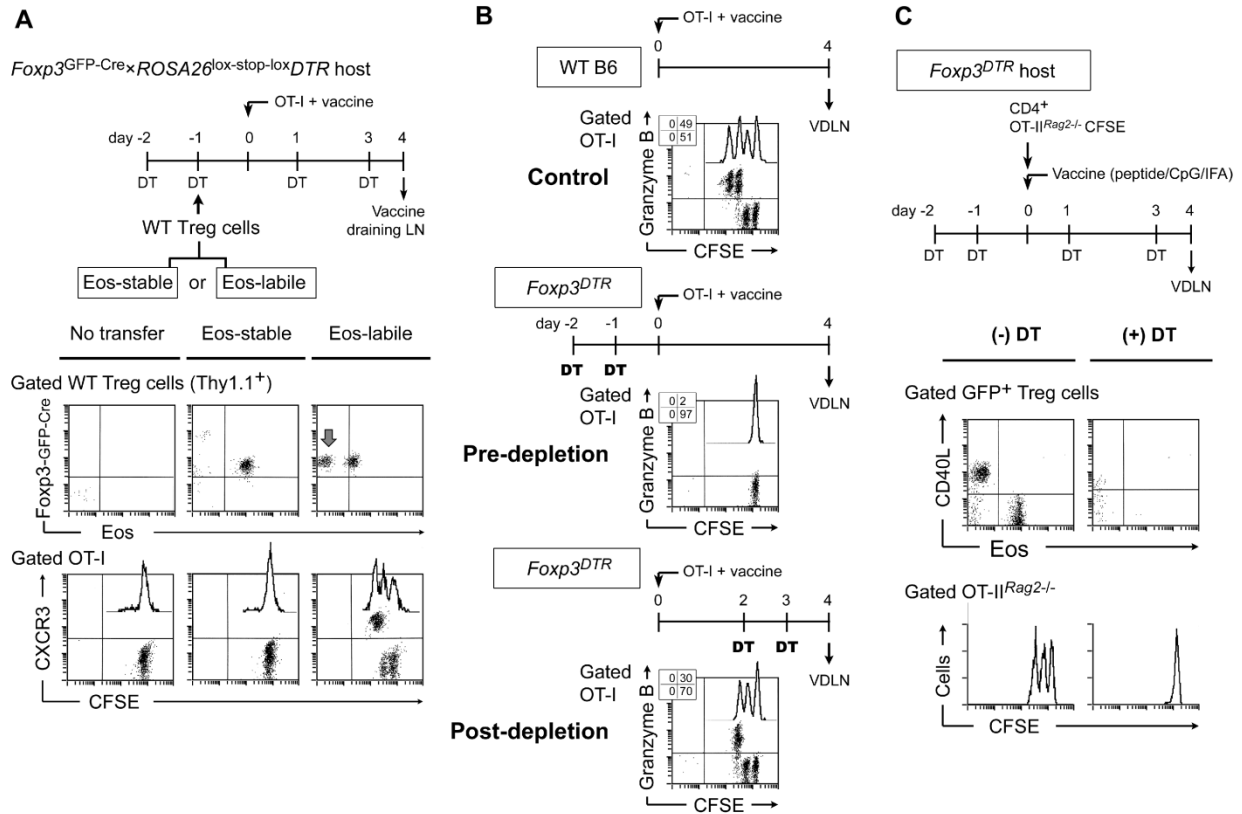


Figure S4. Functional Helper Activity of the Eos-Labile Treg Cell Subset, Related to Figure 4

(A) Adoptive transfer of Eos-labile Treg cells replaces the helper activity that is lost in Treg-depleted mice. *Foxp3*^{GFP-Cre} × *ROSA26*^{lox-stop-lox} *DTR* mice were reconstituted with sorted Eos-labile or Eos-stable Treg cell subsets. (For these functional studies, no CHX was used prior to sorting). All mice were then treated with DT to deplete endogenous (host) Treg cells. Since the transferred Treg cells lacked the DTR transgene they were not affected by DT, and were not depleted. All mice then received OT-I and vaccine, and VDLNs were analyzed on day 4. Without adoptive transfer, Treg cell depletion compromised OT-I priming (left-hand panels), similar to manuscript Figure 4A. Adoptive transfer of the Eos-stable Treg cell subset had no effect on OT-I activation; but transfer of Eos-stable Treg cells rescued OT-I proliferation and differentiation. (In these studies CXCR3 was used as the maturation marker for OT-I differentiation; granzyme B gave identical results).

(B) Help from Treg cells is critical only at the time of initial priming. Manuscript Figure 4C suggested that the key time for help from Treg cells was during the initial priming stage. Consistent with this hypothesis, Figure S4B shows that depletion of Treg cells before vaccination impaired OT-I priming; but depletion 2 days after vaccination had minimal effect. These studies were performed in a second strain of DTR mice (*Foxp3*^{DTR} (Kim et al., 2007)) to confirm that the effect of Treg cell depletion was not peculiar to one DTR model.

(C) CD4⁺ effector T cells are dependent on help from reprogrammed Treg cells in the DTR ablation model. *Foxp3*^{DTR} mice (Kim et al., 2007) received DT as indicated (1 ug i.p./dose) or vehicle control. CD4⁺ OT-II^{Rag2-/-} effector cells, recognizing a peptide of OVA in the context of IA^b (Barnden et al., 1998), were purified by negative-selection bead enrichment, labeled with CFSE, and transferred into the *Foxp3*^{DTR} hosts. All mice were immunized with cognate peptide OVA₃₂₃₋₃₃₉ in CpG+IFA vaccine. After 4 days VDLNs were analyzed for CD40L vs Eos expression in Treg cells, and OT-II^{Rag2-/-} proliferation.

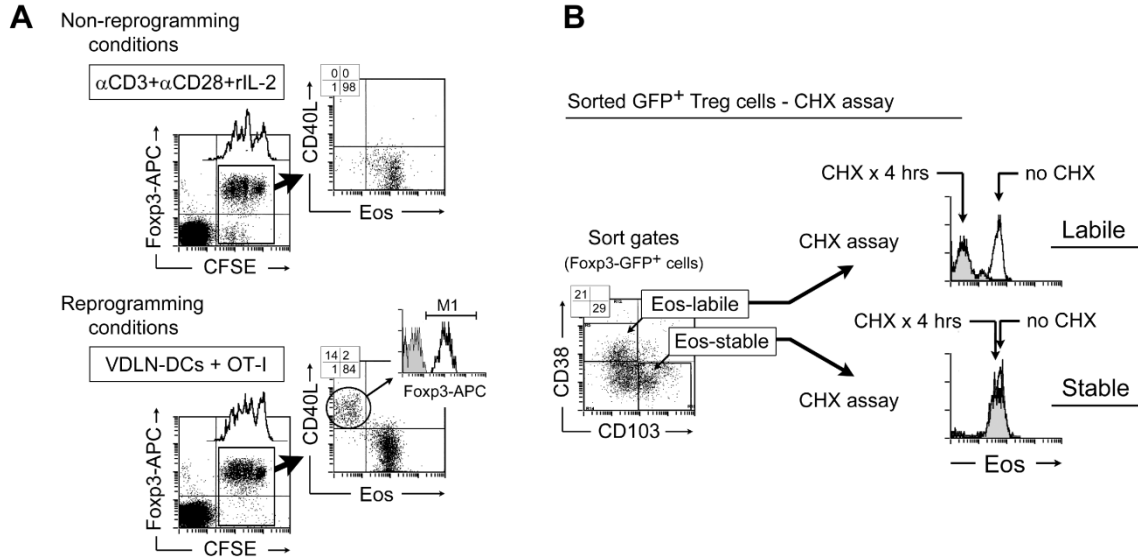


Figure S5. Stability of Foxp3 Expression during Proliferation, and Purity of FACS-Sorted Treg Cell Subsets, Related to Figure 5

(A) Eos-labile Treg cells can undergo proliferation without loss of Foxp3. Sorted B6 Treg cells (CD4⁺CD25⁺) were labeled with CFSE and cultured in vitro for 4 days, either under non-reprogramming conditions (activation with α CD3+ α CD28 mitogen plus rIL-2 and feeder cells), or reprogramming conditions (co-culture with VDLN DCs and OT-I+SIINFEKL, as in manuscript Figure 1C). The superimposed CFSE histograms show that Treg cells proliferated under both conditions, and in each case maintained stable Foxp3 expression while proliferating. This specifically included the reprogrammed Treg cell population (Eos^{NEG} and CD40L⁺) which still remained uniformly Foxp3⁺ (inset histogram, showing Foxp3 expression in reprogrammed cells, versus isotype-matched control antibody in grey).

(B) Efficient separation of Eos-labile and Eos-stable subsets by FACS sorting. *Foxp3*^{GFP} Treg cells were FACS sorted into CD38⁺CD103^{NEG} and CD38^{NEG}CD103⁺ subsets (the same subsets used for adoptive transfer in manuscript Figure 5), and then tested in a 4 hr CHX assay for labile versus stable Eos expression.

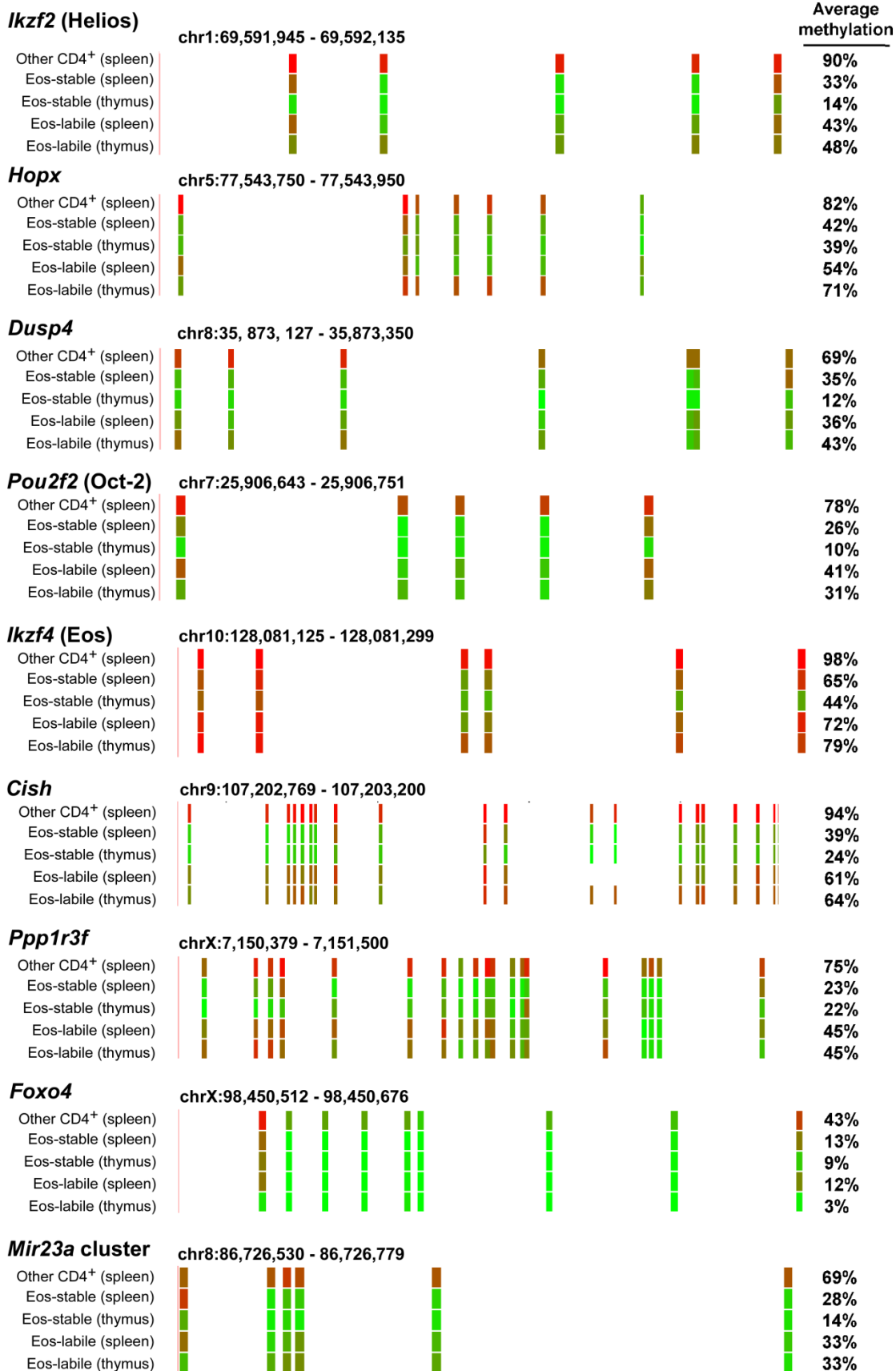


Figure S6. Specific Examples of Differentially Methylated Sites in Eos-Stable Treg Cells, Eos-Labile Treg Cells, and Nonregulatory CD4⁺ Cells, Related to Figure 6

Details of results for selected genes from the genome-wide DNA methylation analysis shown in manuscript Figure 6. Cells from thymus or spleen were pre-treated with CHX for 1 hr, then CD4⁺GFP⁺ Treg cells sorted into Eos-labile (CD38⁺CD103^{NEG}) and Eos-stable (CD38^{NEG}CD103⁺) subsets. As controls, CD4⁺GFP^{NEG} cells (“Other CD4⁺” group) were sorted from spleen. Methylation analysis was performed as described in Supplemental Methods. Examples of informative genes were selected from the hierarchical clustering analysis, based on a methylation pattern that was similar in all of the four Treg cell groups, while all the Treg cells were different from the Other CD4⁺ control. Several of these proved to be genes which are known to be expressed in Treg cells or important in T cell differentiation, such as *Ikzf2* (Helios) (Thornton et al., 2010), *Dusp4* (Haribhai et al., 2011), and *Hopx* (Hawiger et al., 2010).

The tracks shown from top to bottom are: DNA methylation level at each CpG site derived from the bisulfite sequencing reads; RefSeq genes; and conservation score in the UCSC genome browser. Red and green colors indicate methylated and unmethylated CpG sites, respectively. All RRBS sequence data have been submitted to the GEO database (accession number GSE44380).

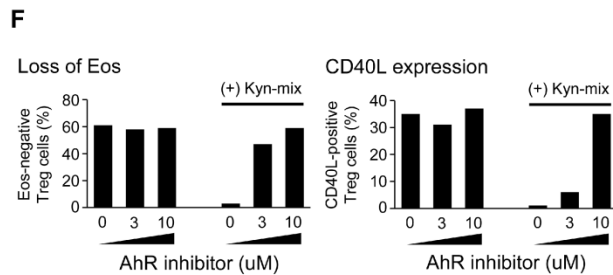
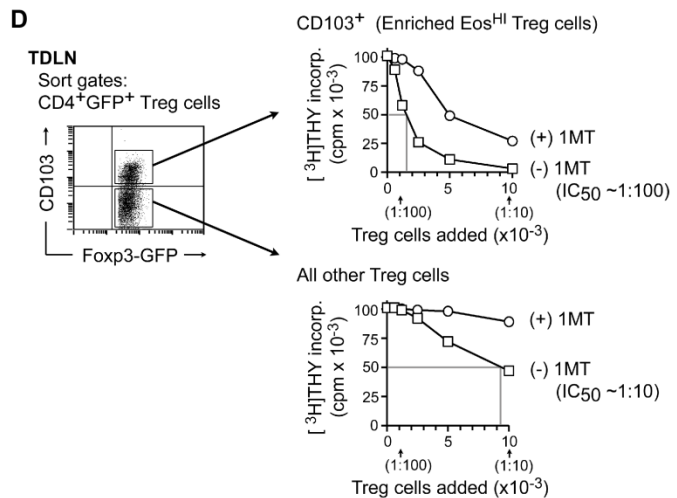
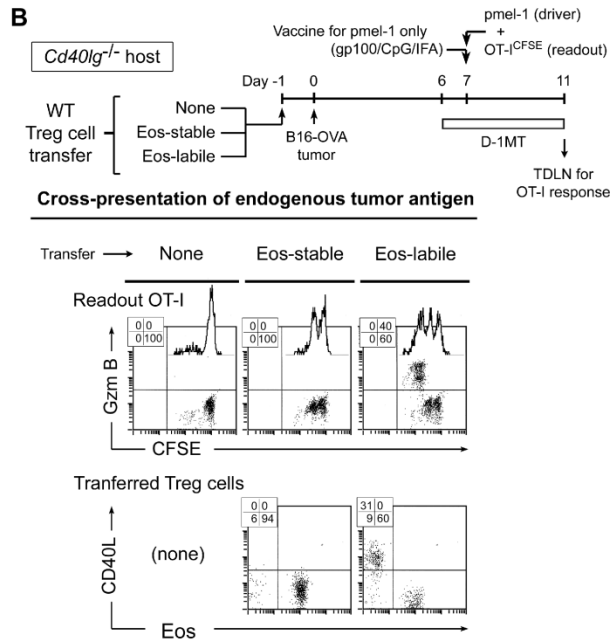
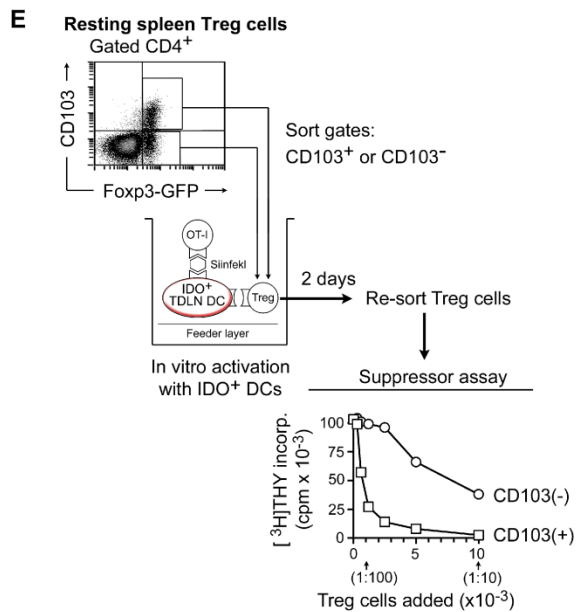
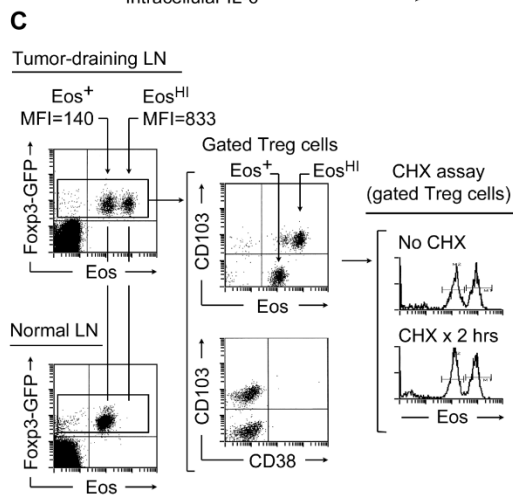
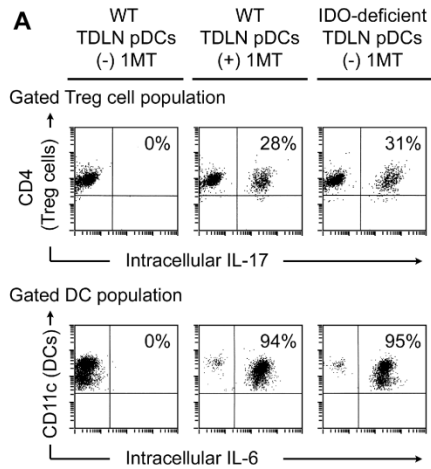


Figure S7. Tumor-Draining LNs Contain a Population of IDO-Activated Eos^{HI} Treg Cells that Mediate Enhanced Suppressor Activity, Related to Figure 7

(A) pDCs from TDLNs of IDO-deficient hosts do not suppress Treg cell reprogramming. B16 melanoma tumors were grown in WT B6 mice or *Ido1*^{-/-} mice (B6 background). Plasmacytoid DCs (pDCs) were isolated from TDLNs, and used in reprogramming co-cultures (as diagramed in Figure S1E, and described in Supplemental Experimental Procedures). The upper row of dot plots shows the gated Treg cell population after 2 days in co-culture, identified based on CD4 expression, with IL-17 used as a marker for Treg cell reprogramming. TDLN pDCs from IDO-sufficient (WT) hosts suppressed Treg cell reprogramming, and this was reversed when the IDO pathway was inhibited with 1MT. However, TDLN pDCs from *Ido1*^{-/-} hosts could not suppress Treg cell reprogramming, even in the absence of 1MT. The lower row of dot-plots shows the pDC population after co-culture, stained for intracellular IL-6. As we have previously reported (Sharma et al., 2009), when TDLN pDCs were from WT hosts, active IDO blocked expression of IL-6 unless 1MT was added; whereas *Ido1*^{-/-} TDLN pDCs expressed IL-6 even without 1MT.

(B) Cross-presentation model: Helper activity of Eos-labile Treg cells licenses effective cross-presentation of endogenous tumor antigen to anti-tumor T cells. CD40L-deficient (*Cd40lg*^{-/-}) host mice received either Eos-labile or Eos-stable Treg cell populations sorted from CD40L-sufficient (WT) *Foxp3*^{GFP} mice. Control hosts received no transfer. All mice were implanted with B16-OVA tumors, which expressed antigen for both pmel-1 and OT-I cells. On day 7 of tumor growth, all mice received adoptive transfer of CFSE-labeled OT-I (the readout cells) and unlabeled pmel-1 (the driver cells). Mice were then immunized with gp100 vaccine to activate the pmel-1, but received no OVA vaccine. Thus, the only source of antigen to activate OT-I was endogenous antigen from the tumors, cross-presented by host DCs. Four days after vaccination, OT-I responses were assessed in TDLN as proliferation by CFSE, and effector differentiation by granzyme B expression.

(C) Suppressive Eos^{HI} Treg cells in TDLNs are preferentially enriched in the CD103⁺ Treg cell population. *Foxp3*^{GFP} host mice were implanted with B16F10 melanoma tumors. On day 7, TDLNs were analyzed for CD103 and CD38 expression. The TDLN cells were also tested in a CHX assay for the presence of Eos-labile Treg cells. The left-hand dot-plots shows that TDLNs contained a population of Eos^{HI} Treg cells that was not present in LNs of mice without tumors. The right-hand dot-plots show that the Eos^{HI} Treg cell population was highly enriched within the CD103⁺ Treg cells. Furthermore, there were virtually no CD38⁺ Treg cells in TDLNs (which, in normal LNs, would be the marker for the Eos-labile, reprogrammable Treg cell population). Consistent with the absence CD38, the CHX assay (right-hand histograms) revealed that virtually all Treg cells in TDLNs were Eos-stable and none were Eos-labile (i.e., no loss of Eos occurred after CHX).

(D) Sorted CD103⁺ Treg cells from TDLNs (corresponding to the Eos^{HI} Treg cells) mediate potent suppressor activity in vitro. We have previously shown that Treg cells isolated from TDLNs are constitutively activated for potent suppressor activity, and that much of this activation is caused by IDO (Sharma et al., 2007). To ask whether the highly suppressive Treg cells in TDLNs corresponded to the Eos^{HI} population, *Foxp3*^{GFP} host mice bearing established B16F10 tumors were treated with gp100-specific pmel-1 cells plus hgp100+CpG+IFA vaccine, and received either 1MT or vehicle control in drinking water, as shown. Four days after vaccination, Treg cells from TDLNs were sorted based on CD103 expression as a proxy marker for Eos^{HI} cells (the Treg cells could not be sorted on Eos itself because Eos is an intracellular

antigen; however, as shown in the preceding panel, the CD103⁺ population corresponded closely to the Eos^{HI} Treg cells). Sorted CD103⁺ (Eos^{HI}) Treg cells and CD103^{NEG} Treg cells (all others) were then added to allogeneic readout assays (1×10⁵ HY-specific T cells plus CBA spleen cells and cognate peptide, as previously described (Sharma et al., 2007)). For these assays, a peptide-specific allogeneic readout system was used (instead of anti-CD3 mitogen) so that there would not be any non-specific mitogen-induced activation of the Treg cells in the readout assay itself (Thornton and Shevach, 2000). Thus, any Treg cell suppressor activity in this assay reflected a constitutive functional activation, acquired in vivo in the TDLN. Proliferation of readout T cells was measured after 72 hrs by thymidine incorporation. The approximate IC50 values are shown interpolated for the two different Treg cell populations, and comparing mice with and without 1MT treatment. The CD103⁺ Treg cells (enriched Eos^{HI}) were markedly more suppressive than the other Treg cells in TDLNs, and the level of suppression was reduced by 1MT treatment in vivo.

(E) The highly suppressive Treg cells induced by IDO derive from the Eos-stable (CD103⁺) population of resting Treg cells. Resting Treg cells from spleens of naive *Foxp3*^{GFP} donors (without tumors) were sorted into CD103⁺ and CD103^{NEG} fractions, then separately activated for 2 days in co-cultures with IDO-expressing DCs sorted from TDLNs (using co-cultures similar to manuscript Figure 7A). Following activation, the Treg cells were recovered by sorting for CD4⁺ cells, and tested for functional suppressor activity by thymidine-incorporation assay as in the preceding panel. The Treg cells derived from the original CD103⁺ fraction became potently suppressive in response to IDO.

(F) The effect of KYN metabolites on Treg cell reprogramming is mediated via the AhR. To test whether KYN metabolites exerted their effect on Eos via the AhR, we added the pharmacologic AhR inhibitor CH223191 (Zhao et al., 2010) to reprogramming co-cultures with and without added KYN metabolites (similar to manuscript Figure 7D). Reprogramming was quantitated as the percentage of Treg cells that lost Eos (upper panels) and acquired CD40L expression (lower panels) by FACS analysis. The presence of KYN metabolites abrogated reprogramming; the addition of the CH223191 AhR inhibitor blocked the effect of KYN metabolites and restored reprogramming, in a dose-dependent fashion.

Supplemental Experimental Procedures

Reagents and 1MT

1-methyl-D-tryptophan (1MT) was supplied by NewLink Genetics Inc. (Ames, IA) and administered in drinking water at 2 mg/ml as previously described (Sharma et al., 2007). For in vitro studies, 1MT was dissolved in alkaline pH as described (Munn et al., 2005) and diluted in PBS at final pH 7.4. AhR inhibitor CH223191 was obtained from EMD-Calbiochem. Neutralizing anti-IL-6 (cat. # AF-406-NA, R&D Systems) was used at 100 ug/ml. Recombinant mouse IL-6 was from R&D systems. Diphtheria toxin (Sigma) was given at 1 ug/dose i.p.

Mouse Strains

Foxp3^{GFP} mice (Fontenot et al., 2005), bearing a *Foxp3*-GFP fusion protein replacing the normal coding region of the *Foxp3* locus, were the gift of Alexander Rudensky and were inbred on the B6 background. This *Foxp3*-GFP fusion protein had the important advantage that it ensured complete fidelity of the GFP marker, which was crucial when tracking reprogrammed Treg cells. However, the *Foxp3*-GFP fusion construct can affect some biologic functions of *Foxp3* (Bettini et al., 2012). Therefore, key results were always confirmed in WT mice without any reporter gene (using *Foxp3* antibody staining). Results were further confirmed in a second reporter strain with a BAC-transgenic GFP-Cre fusion protein under the *Foxp3* promoter (Zhou et al., 2009; Zhou et al., 2008) (obtained from Jackson Laboratories, NOD/ShiLt-Tg(*Foxp3*-EGFP/cre)1Jbs/J, and back-crossed in our colony onto the B6 background).

For DTR experiments, *Foxp3*^{GFP-Cre} mice, as above, were crossed to mice bearing a human diphtheria-toxin receptor transgene behind a floxed STOP codon under the *ROSA26* promoter (*ROSA26*^{lox-stop-lox}*DTR*) (Buch et al., 2005) (C57BL/6-*Gt(ROSA)26Sor*^{tm1(HBEGF)Awai}/J, Jackson Laboratories). The F1 offspring (*Foxp3*^{GFP-Cre} × *ROSA26*^{lox-stop-lox}*DTR*) expressed DTR selectively on Treg cells, as previously described (Sharma et al., 2010). To confirm these DTR studies, a second strain of *Foxp3*^{DTR} mice, with a DTR-GFP fusion construct knocked-in to the 3'-UTR of the *Foxp3* gene (but with a normal *Foxp3* coding sequence) were used (gift of Dr. Rudensky (Kim et al., 2007)).

Rag2^{-/-} mice (B6.129S6-*Rag2*^{tm1Fwa} N12) and OT-II^{*Rag2*^{-/-}} mice (B6.129S6-*Rag2*^{tm1Fwa} Tg(*TcraTcrb*)425Cbn, recognizing a peptide of OVA in the context of IA^b (Barnden et al., 1998) and bred onto the *Rag2*^{-/-} background) were from Taconic. The following strains were obtained from Jackson Laboratories and bred in our colony: OT-I mice (CD8⁺, recognizing the SIINFEKL peptide of ovalbumin on H2K^b (Hogquist et al., 1994)); pmel-1 mice (Overwijk et al., 2003), strain B6.Cg-*Thy1*^a/CyTg(*TcraTcrb*)8Rest/J, recognizing a peptide from human gp100 (cross-reactive with mouse gp100); *Cd40lg*^{-/-} mice (Renshaw et al., 1994), strain B6.129S2-*Cd40lg*^{tm1Imx}/J; and *Il6*^{-/-} mice (B6.129S2-*Il6*^{tm1Kopf}/J) (Kopf et al., 1994).

Vaccine Preparation and Vaccination

CpG-1826 (phosphorothioate oligo 5'-TCCATGACGTTCCCTGAGCTT-3') was synthesized based on the published sequence (Chu et al., 1997) by Tri-link Biotechnologies. Whole OVA protein was obtained from Sigma (catalog #A-5503). Human gp100₂₅₋₃₃ (KVPRNQDWL) was synthesized by Southern Biotechnology based on the published sequence (Overwijk et al., 2003). OT-II peptide (OVA₃₂₃₋₃₃₉) was from GenScript, Piscataway, NJ. Vaccines were prepared by emulsifying 100 ug of whole OVA protein (Sigma), or 25 ug of each peptide, with 50 ug

CpG-1826 in incomplete Freund's adjuvant (IFA, Sigma F-5506) and administered in the footpad.

Mice received 1×10^6 OT-I or pmel-1 spleen cells (enriched by CD8⁺ magnetic beads) or OT-II^{Rag2^{-/-}} (enriched for CD4 by negative-selection beads) via tail-vein. Vaccine was administered in the footpad, and popliteal LNs removed on day 4. Where indicated, mice received CD40-agonist antibody (clone FGK45, 250 ug i.p. on the day of vaccination and 100 ug i.p. 2 days later), and recombinant mouse IL-2 (1 ug i.p. every 12 hrs).

Influenza Virus Infection

Stocks of HKx31 (X31, H3N2) influenza virus were propagated in embryonated chicken eggs and provided by Ralph Tripp in University of Georgia. Mice were anesthetized with isoflurane and infected with X31 diluted in PBS with 0.1% endotoxin free, Ig free BSA (Gemini Bio-products, Calabasas, California) via intranasal inoculation. To extract immune cells in the lungs, mice were perfused and lung was digested in 5 ml 400 units/ml of collagenase (Worthington Biochemical, Lakewood, NJ). Immune cells were then enriched by centrifugation in 40% Percoll (GE Healthscience).

Treg Cell In Vitro Cocultures

The Treg cell + DC co-culture system was used as described previously (Sharma et al., 2009). To obtain activated DCs from VDLNs, B6 donor mice were immunized with OVA+CpG+IFA vaccine plus adoptive transfer of OT-I cells, then CD11c⁺ DCs were FACS-sorted from popliteal LNs 2 days after immunization, and added to co-cultures at 5×10^3 cells/well. Resting Treg cells (range 5×10^3 to 2×10^4 /well) were sorted as CD4⁺GFP⁺ cells from spleens of *Foxp3^{GFP}* mice. To recapitulate the milieu of an activated LN, 1×10^5 sorted CD8⁺ OT-I spleen cells and 100 nM cognate SIINFEKL antigen were added. The data shown used OT-I effector cells in the assay, but CD4⁺ effector cells also drove reprogramming. All cultures received a feeder layer of 1×10^5 T cell-depleted B6 spleen cells (CD4^{NEG}CD8^{NEG}) to maintain viability of the sorted populations, as previously described (Sharma et al., 2007). All cells populations were mechanically disaggregated through 40 um mesh.

The co-culture system was designed such that the only cells expressing CD4 were the original Treg population; thus, the Tregs could always be unambiguously identified irrespective of any subsequent change in CD25 or Foxp3.

For co-cultures using IDO⁺ DCs from TDLNs, plasmacytoid DCs were enriched from TDLNs of B16F10 tumors (day 7-11) by sorting for CD11c⁺B220⁺ cells. This fraction from TDLNs contained many IDO⁺ pDCs, as previously described (Sharma et al., 2007)). In general, cells from TDLNs were potently inhibitory for Treg cell reprogramming; this could be reduced somewhat by using less advanced tumors (before day 11), and by using the pDC fraction instead of total DCs.

For kynurenine-metabolite studies, a mixture was used comprising kynurenic acid, 3-hydroxykynurenine, anthranilic acid, 3-hydroxyanthranilic acid and quinolinate (all from Sigma) at a final concentration of 10 uM for each compound (50 uM total metabolites).

For α CD3-induced Treg cell activation, CD4⁺GFP⁺ Treg cells from *Foxp3^{GFP}* mice were cultured with T-depleted spleen cell feeder layer (CD4^{NEG}CD8^{NEG}), as described by Shevach and colleagues (Thornton et al., 2004), in the presence of 0.1 ug/ml α CD3 mAb and 10 ng/ml rhIL-2.

After 2 days cultures were harvested and Treg cells recovered by sorting for CD4⁺ cells (by design the Treg cells were the only CD4⁺ cells in the cultures and so could be readily recovered).

Treg Cell Suppression Assay

To measure functional Treg cell suppression, Treg cells were sorted and added in varying numbers to readout assays comprising 5×10^4 sorted non-Treg cell effector cells, 1×10^5 T-depleted spleen cells, and 0.1 ug/ml α CD3 mitogen. Proliferation of readout T cells was measured after 72 hrs by thymidine incorporation assay. Suppression was confirmed using both CD4⁺ and CD8⁺ target cells. When the property of interest was constitutive (spontaneous) suppression, an antigen-specific readout assay was used as described in Figure 7D.

Cycloheximide Assay

Thymus or LN cells were mechanically disaggregated and incubated in complete medium for 1-4 hrs in the presence of 20 ug/ml CHX (Sigma). Control cultures received medium with vehicle alone. At the end of incubation cells were stained for Treg cell markers and intracellular Eos expression.

Antibodies and FACS Staining

Treg cells were fragile during staining. We found that it was important to disaggregate LNs rapidly (passing once through a 40 um mesh) and stain quickly using short incubation times (10 min on ice). Nonspecific background was lowest using the fixation-permeabilization reagent from eBioscience (Cat. #00-5521). Our intracellular staining method for Treg cells was modified from published methods (Bettelli et al., 2006), using lower concentration of PMA to reduce background staining, and incubating for 4 hrs, as described (Sharma et al., 2010). When using a commercial PMA+ionomycin kit (BD-Pharmingen, Cat. #550583), we used one-tenth (1/10) the recommended concentration of the PMA+ionomycin reagent, supplemented with GolgiPlug reagent to the recommended full-strength concentration. Concentrations of PMA and ionomycin were titrated empirically for each reagent to produce low background in resting CD4⁺ spleen cells. Intracellular staining of DCs for IL-6 was performed similarly, following incubation for 4 hrs in PMA+ionomycin+brefeldin A. All cells were acquired with doublet discrimination.

To minimize artifactual difficulties in staining for Foxp3 after reprogramming (see Figure S1F, above), we avoided PMA activation when staining for Foxp3, and used brief staining incubations (10 min. on ice) and short washes (3 min). With these modifications, Foxp3 antibody staining was concordant with the GFP reporter genes.

Antibodies were as follows: Goat anti-Eos (sc-132308) and rabbit anti-Eos (sc-292209) were from Santa Cruz Biotechnology used at 2 ug/ml, followed by cross-adsorbed secondary donkey anti-goat-APC (705-136-147) or donkey anti-rabbit-PE (711-106-152) from Jackson Immunoresearch. The following were from BD-Pharmingen: phospho-STAT3 (clone M59-50) used with the manufacturer's reagents according to Phosflow Protocol #1; CD69 (H1.2F3); CD4 (GK1.5); CD8 α (53-6.7); CD80 (16.10A1); CD86 (GL1). Antibodies from eBioscience were: anti-Foxp3 (clone FJK-16s), anti-IL-6 (clone MP5-20F3), anti-CD38 (clone 90), anti-CD103 (Ber-ACT8), anti-IL-2 (JES6-5H4); anti-IL-17A (17B7); anti-CD40L (MR1, used at 1:50 dilution); anti-granzyme B (16G6); anti-Foxp3 (clones JFK-16 and NNRF-30). Antibody against CXCR3 was from R&D Systems (220803).

Retroviral Transduction

Mouse Eos was cloned into the pMIG vector (MSCV-IRES-GFP) (Hawley et al., 1992) as previously described (Pan et al., 2009). Producer cells (293T) were co-transfected with pMIG-Eos plus packaging plasmid pCL-Eco (Imgenex) using FuGene HD. Day 2 supernatants were titered for infectivity using 3T3 cells. Control (GFP-only) virus was produced by using empty pMIG vector plus packaging plasmid.

Transduction of resting Treg cells was performed using Treg+DC co-cultures (as described in manuscript figure 1C), but with delayed addition of SIINFEKL peptide. Treg cells were prepared from B6 mice as CD4⁺CD25⁺ cells by FACS sorting, and added to resting (unactivated) co-cultures comprising VDLN DCs plus OT-I and feeder layer (but without SIINFEKL peptide). Co-cultures were incubated overnight with virus-containing supernatant from producer cells (either Eos-GFP virus or control GFP-only virus) in the presence of 8 ug/ml polybrene and 1 mM HEPES. After 18 hrs the cells were washed, medium was changed to standard culture medium, and SIINFEKL was added (reprogramming conditions). After 2 more days the cultures were analyzed by FACS.

For subsequent adoptive-transfer studies, co-cultures were harvested after transduction (3 days total culture) and Treg cells recovered by magnetic-bead sorting for CD4. (By design the Treg cells were the only CD4⁺ cells in the co-cultures, so they could be readily recovered.) Enriched Treg cells were then adoptively transferred into new hosts.

Methylation Analysis: Reduced Representation Bisulfite Sequencing (RRBS)

RRBS was performed according to a previously published protocol (Gu et al., 2010; Meissner et al., 2008) with minor modifications. For each sample, 200-500 ng genomic DNA was digested overnight with 40 units of MspI (New England Biolabs, Ipswich, MA). The digested DNA fragments were end-repaired, A-tailed and ligated to methylated Illumina adapters. The ligation products were subjected to size-selection on a 3% NuSieve 3:1 agarose gel. Slices of 160-350bp were excised from the gel as suggested (Gu et al., 2010; Meissner et al., 2008). Bisulfite treatment was conducted using the EZ DNA methylation kit (Zymo Research, Irvine, CA) according to manufacturer's protocol. The final libraries were generated using 5 µl bisulfite-converted template in a 14-cycle PCR amplification using the PfuTurbo Cx Hotstart polymerase (Agilent Technologies, Santa Clara, CA). The libraries were sequenced using an Illumina Genome Analyzer IIx (Illumina, San Diego, CA) with a read length of 100 bp.

The raw sequencing reads were trimmed to remove sequencing adapters, low quality bases (Q<67 in Illumina 1.5) in the 3' end and ambiguous bases in both ends. To map the sequencing reads from RRBS, the mouse genome (mm9) was indexed by converting all C's and G's to T's and A's, respectively, which results in two different reference databases representing both strands. The cleaned reads was used to map to each of the two reference databases using Bowtie (Langmead et al., 2009) after converting all C's to T's. For each read, an in-house script computed the best of all alignments for the different loci using two different reference databases based on the number of mismatches after realigning the original read and reference sequences. Another in-house script determined the methylation status of each cytosine residue by comparing the bisulfite-converted sequence to the reference sequence. The third script piled reads for each cytosine in the reference genome and counted the numbers of reads that contained methylated and unmethylated cytosines, respectively. Finally the methylation of each CpG site was defined as the fraction of methylated reads to that of methylated and unmethylated reads combined.

CpGs with < 5 reads were filtered out for further analyses. We used windows of length 200bp with an overlap of 100bp between to identify differentially methylated regions (DMRs) by summing the numbers of methylated and unmethylated CpGs in reads, respectively. The windows containing fewer than 5 CpGs were filtered out for further analysis. The DMRs between two samples, e.g., EOS-labile versus Non-Treg cells, were identified by Fisher's exact tests with an FDR < 0.01 and a methylation ratio difference > 0.25. After performing the pair wise fisher exact test, the overlapping windows were combined and only non-overlapping DMRs were used for the cluster analysis. Cluster analysis was performed in R using the DMRs identified by the Fisher's exact test. The DMRs were compared with RefSeq genes, CpG islands, and repeats in the UCSC genome browser and classified into functional categories such as promoters, 5'-UTRs, exons, 3'-UTRs, and 3' ends of the RefSeq genes.

The raw and analyzed sequencing data from this study has been submitted to NCBI Gene Expression Omnibus (GEO) database, accession number GSE44380.

Quantitative Reverse-Transcriptase PCR

Treg cell subsets were isolated by FACS sorting. Total RNA was extracted using RNeasy Mini Kit (Qiagen, Valencia CA). One step RT-PCR was performed using the SYBR Green 1 Light Cycler RNA Amplification KIT (Roche Diagnostics, Mannheim Germany) on a Light Cycler 2.0 (Roche Diagnostics) using Eos, Foxp3 and Gapdh primers. Results were normalized to Gapdh expression. PCR amplification was performed in a total volume of 20 µl, which contained 2 µl of total RNA, 4.0 µl of stock SYBR Green 1 reaction mix (5x stock), 6 mM MgCl₂ (EOS and Gapdh) or 7 mM MgCl₂ (Foxp3), 0.25 µM (Gapdh) to 0.30 µM (EOS and Foxp3) of primer mix, 0.4 µl of RT-PCR Enzyme Mix. For each reaction, a control RNA sample without RT-PCR Enzyme Mix and a sample with PCR water only with RT-PCR Enzyme Mix were run as negative controls. Each PCR amplification was performed under the following conditions: 30 min at 55°C for RT, followed by denaturation at 95°C for 30 sec, then PCR as follows:

EOS: 45 cycles of denaturation at 95°C for 5 sec, annealing at 68°C for 10 sec and extension at 72°C for 17 sec.

Foxp3: 30 min at 55°C for RT, 45 cycles denaturation at 95°C, annealing at 53°C for 5 sec and extension at 72°C for 10 sec.

Gapdh: 20 min at 55°C for reverse transcription, 45 cycles of denaturation at 95°C for 30 sec, annealing at 60°C for 10 sec and extension at 72°C for 8 sec.

Primers: *EOS*: Forward 5'-CGGCATCCGGCTACCCAACG-3'

Reverse 5'-AGGTCACGGATTCATCACCTGGC-3'.

Foxp3: Forward 5'-CACCTATGCCACCCTTATC-3'

Reverse 5'-TCCTCTTCTTGCGAAACTC-3'

Gapdh: Forward 5'-GTTGTCTCCTGCGACTTCA-3'

Reverse 5'-GTGGTCCAGGGTTTCTTACT-3'

Tumor Studies

The B16F10 cell line was from ATCC. Tumor implantation was performed as described (Sharma et al., 2007), using 1×10⁶ cells in order to ensure rapid tumor growth and immune suppression. Tumor area was measured at necropsy on day 11 as the product of orthogonal diameters.

Supplemental References

- Avitahl, N., Winandy, S., Friedrich, C., Jones, B., Ge, Y., and Georgopoulos, K. (1999). Ikaros sets thresholds for T cell activation and regulates chromosome propagation. *Immunity* 10, 333-343.
- Barnden, M.J., Allison, J., Heath, W.R., and Carbone, F.R. (1998). Defective TCR expression in transgenic mice constructed using cDNA-based alpha- and beta-chain genes under the control of heterologous regulatory elements. *Immunol. Cell Biol.* 76, 34-40.
- Bettelli, E., Carrier, Y., Gao, W., Korn, T., Strom, T.B., Oukka, M., Weiner, H.L., and Kuchroo, V.K. (2006). Reciprocal developmental pathways for the generation of pathogenic effector TH17 and regulatory T cells. *Nature* 441, 235-238.
- Bettini, M.L., Pan, F., Bettini, M., Finkelstein, D., Rehg, J.E., Floess, S., Bell, B.D., Ziegler, S.F., Huehn, J., Pardoll, D.M., and Vignali, D.A. (2012). Loss of epigenetic modification driven by the Foxp3 transcription factor leads to regulatory T cell insufficiency. *Immunity* 36, 717-730.
- Buch, T., Heppner, F.L., Tertilt, C., Heinen, T.J., Kremer, M., Wunderlich, F.T., Jung, S., and Waisman, A. (2005). A Cre-inducible diphtheria toxin receptor mediates cell lineage ablation after toxin administration. *Nat Methods* 2, 419-426.
- Chu, R.S., Targoni, O.S., Krieg, A.M., Lehmann, P.V., and Harding, C.V. (1997). CpG oligodeoxynucleotides act as adjuvants that switch on T helper 1 (Th1) immunity. *J. Exp. Med.* 186, 1623-1631.
- Fontenot, J.D., Rasmussen, J.P., Williams, L.M., Dooley, J.L., Farr, A.G., and Rudensky, A.Y. (2005). Regulatory T cell lineage specification by the forkhead transcription factor foxp3. *Immunity* 22, 329-341.
- Gu, H., Bock, C., Mikkelsen, T.S., Jager, N., Smith, Z.D., Tomazou, E., Gnirke, A., Lander, E.S., and Meissner, A. (2010). Genome-scale DNA methylation mapping of clinical samples at single-nucleotide resolution. *Nat Methods* 7, 133-136.
- Haribhai, D., Williams, J.B., Jia, S., Nickerson, D., Schmitt, E.G., Edwards, B., Ziegelbauer, J., Yassai, M., Li, S.H., Relland, L.M., *et al.* (2011). A requisite role for induced regulatory T cells in tolerance based on expanding antigen receptor diversity. *Immunity* 35, 109-122.
- Hawiger, D., Wan, Y.Y., Eynon, E.E., and Flavell, R.A. (2010). The transcription cofactor Hopx is required for regulatory T cell function in dendritic cell-mediated peripheral T cell unresponsiveness. *Nat. Immunol.* 11, 962-968.
- Hawley, R.G., Fong, A.Z., Burns, B.F., and Hawley, T.S. (1992). Transplantable myeloproliferative disease induced in mice by an interleukin 6 retrovirus. *J Exp Med* 176, 1149-1163.
- Hogquist, K.A., Jameson, S.C., Heath, W.R., Howard, J.L., Bevan, M.J., and Carbone, F.R. (1994). T cell receptor antagonist peptides induce positive selection. *Cell* 76, 17-27.
- Kim, J.M., Rasmussen, J.P., and Rudensky, A.Y. (2007). Regulatory T cells prevent catastrophic autoimmunity throughout the lifespan of mice. *Nat Immunol* 8, 191-197.
- Kopf, M., Baumann, H., Freer, G., Freudenberg, M., Lamers, M., Kishimoto, T., Zinkernagel, R., Bluethmann, H., and Kohler, G. (1994). Impaired immune and acute-phase responses in interleukin-6-deficient mice. *Nature* 368, 339-342.

- Langmead, B., Trapnell, C., Pop, M., and Salzberg, S.L. (2009). Ultrafast and memory-efficient alignment of short DNA sequences to the human genome. *Genome biology* 10, R25.
- Malavasi, F., Deaglio, S., Funaro, A., Ferrero, E., Horenstein, A.L., Ortolan, E., Vaisitti, T., and Aydin, S. (2008). Evolution and function of the ADP ribosyl cyclase/CD38 gene family in physiology and pathology. *Physiol. Rev.* 88, 841-886.
- Meissner, A., Mikkelsen, T.S., Gu, H., Wernig, M., Hanna, J., Sivachenko, A., Zhang, X., Bernstein, B.E., Nusbaum, C., Jaffe, D.B., *et al.* (2008). Genome-scale DNA methylation maps of pluripotent and differentiated cells. *Nature* 454, 766-770.
- Munn, D.H., Sharma, M.D., Baban, B., Harding, H.P., Zhang, Y., Ron, D., and Mellor, A.L. (2005). GCN2 kinase in T cells mediates proliferative arrest and anergy induction in response to indoleamine 2,3-dioxygenase. *Immunity* 22, 633-642.
- Orabona, C., Grohmann, U., Belladonna, M.L., Fallarino, F., Vacca, C., Bianchi, R., Bozza, S., Volpi, C., Salomon, B.L., Fioretti, M.C., *et al.* (2004). CD28 induces immunostimulatory signals in dendritic cells via CD80 and CD86. *Nat Immunol* 5, 1134-1142.
- Overwijk, W.W., Theoret, M.R., Finkelstein, S.E., Surman, D.R., de Jong, L.A., Vyth-Dreese, F.A., DelleMijn, T.A., Antony, P.A., Spiess, P.J., Palmer, D.C., *et al.* (2003). Tumor regression and autoimmunity after reversal of a functionally tolerant state of self-reactive CD8+ T cells. *J. Exp. Med.* 198, 569-580.
- Pan, F., Yu, H., Dang, E.V., Barbi, J., Pan, X., Grosso, J.F., Jinasena, D., Sharma, S.M., McCadden, E.M., Getnet, D., *et al.* (2009). Eos mediates Foxp3-dependent gene silencing in CD4+ regulatory T cells. *Science* 325, 1142-1146.
- Quintana, F.J., Jin, H., Burns, E.J., Nadeau, M., Yeste, A., Kumar, D., Rangachari, M., Zhu, C., Xiao, S., Seavitt, J., *et al.* (2012). Aiolos promotes T(H)17 differentiation by directly silencing Il2 expression. *Nat. Immunol.*
- Renshaw, B.R., Fanslow, W.C., 3rd, Armitage, R.J., Campbell, K.A., Liggitt, D., Wright, B., Davison, B.L., and Maliszewski, C.R. (1994). Humoral immune responses in CD40 ligand-deficient mice. *J Exp Med* 180, 1889-1900.
- Rudra, D., Deroos, P., Chaudhry, A., Niec, R.E., Arvey, A., Samstein, R.M., Leslie, C., Shaffer, S.A., Goodlett, D.R., and Rudensky, A.Y. (2012). Transcription factor Foxp3 and its protein partners form a complex regulatory network. *Nat. Immunol.* 13, 1010-1019.
- Sharma, M.D., Baban, B., Chandler, P., Hou, D.Y., Singh, N., Yagita, H., Azuma, M., Blazar, B.R., Mellor, A.L., and Munn, D.H. (2007). Plasmacytoid dendritic cells from mouse tumor-draining lymph nodes directly activate mature Treg cells via indoleamine 2,3-dioxygenase. *J. Clin. Invest.* 117, 2570-2582.
- Sharma, M.D., Hou, D.Y., Baban, B., Koni, P.A., He, Y., Chandler, P.R., Blazar, B.R., Mellor, A.L., and Munn, D.H. (2010). Reprogrammed Foxp3(+) Regulatory T Cells Provide Essential Help to Support Cross-presentation and CD8(+) T Cell Priming in Naive Mice. *Immunity* 33, 942-954.
- Sharma, M.D., Hou, D.Y., Liu, Y., Koni, P.A., Metz, R., Chandler, P., Mellor, A.L., He, Y., and Munn, D.H. (2009). Indoleamine 2,3-dioxygenase controls conversion of Foxp3+ Treg cells to TH17-like cells in tumor-draining lymph nodes. *Blood* 113, 6102-6111.
- Thornton, A.M., Korty, P.E., Tran, D.Q., Wohlfert, E.A., Murray, P.E., Belkaid, Y., and Shevach, E.M. (2010). Expression of Helios, an Ikaros transcription factor family member, differentiates thymic-derived from peripherally induced Foxp3+ T regulatory

- cells. *J Immunol* *184*, 3433-3441.
- Thornton, A.M., Piccirillo, C.A., and Shevach, E.M. (2004). Activation requirements for the induction of CD4+CD25+ T cell suppressor function. *Eur. J. Immunol.* *34*, 366-376.
- Thornton, A.M., and Shevach, E.M. (2000). Suppressor effector function of CD4+CD25+ immunoregulatory T cells is antigen nonspecific. *J. Immunol.* *164*, 183-190.
- Zhao, B., Degroot, D.E., Hayashi, A., He, G., and Denison, M.S. (2010). CH223191 is a ligand-selective antagonist of the Ah (Dioxin) receptor. *Toxicol. Sci.* *117*, 393-403.
- Zhou, X., Bailey-Bucktrout, S.L., Jeker, L.T., Penaranda, C., Martinez-Llordella, M., Ashby, M., Nakayama, M., Rosenthal, W., and Bluestone, J.A. (2009). Instability of the transcription factor Foxp3 leads to the generation of pathogenic memory T cells in vivo. *Nat. Immunol.* *10*, 1000-1007.
- Zhou, X., Jeker, L.T., Fife, B.T., Zhu, S., Anderson, M.S., McManus, M.T., and Bluestone, J.A. (2008). Selective miRNA disruption in T reg cells leads to uncontrolled autoimmunity. *J Exp Med* *205*, 1983-1991.